

# Common and lifestyle-specific traits of mycorrhizal root metabolome reflect ecological strategies of plant–mycorrhizal interactions

Mengxue Xia<sup>1</sup>  | Vidya Suseela<sup>1</sup>  | M. Luke McCormack<sup>2</sup>  | Peter G. Kennedy<sup>3</sup>  | Nishanth Tharayil<sup>1</sup> 

<sup>1</sup>Department of Plant & Environmental Sciences, Clemson University, Clemson, South Carolina, USA

<sup>2</sup>Center for Tree Science, The Morton Arboretum, Lisle, Illinois, USA

<sup>3</sup>Department of Plant and Microbial Biology, University of Minnesota, St Paul, Minnesota, USA

**Correspondence**  
Mengxue Xia  
Email: [xiamengxue12@gmail.com](mailto:xiamengxue12@gmail.com)

Nishanth Tharayil  
Email: [ntharay@clemson.edu](mailto:ntharay@clemson.edu)

**Funding information**  
National Science Foundation, Grant/Award Number: DEB 1753621 and DEB 1754679; National Institute of Food and Agriculture, Grant/Award Number: 2021-70410-35296; Clemson University, Grant/Award Number: 7096

**Handling Editor:** Pierre Mariotte

## Abstract

1. Mycorrhizas are widespread below-ground symbioses formed between plant roots and soil fungi. This plant–fungal partnership impacts terrestrial ecosystems by mediating plant performance and biogeochemical processes. The influence of mycorrhizas on plant and ecosystem functioning is ultimately driven by the biological processes that regulate plant–mycorrhizal interactions. Although convergent patterns in morphological and genetic traits of mycorrhizas have been well-documented and reflect key selection forces that shape the biology of mycorrhizas, generalizable traits of mycorrhizal-associated root metabolome, which are more intimately linked to plant and ecosystem functioning, remain unexplored.
2. Here, we compared mycorrhizal-associated metabolome alterations across multiple plant–mycorrhizal fungus combinations. Specifically, we inoculated a phylogenetically diverse set of temperate tree species with either arbuscular mycorrhizal or ectomycorrhizal fungi (the two major mycorrhizal lifestyles). Using comprehensive metabolomics approaches, we then assessed the metabolome in mycorrhizal and non-mycorrhizal roots and the corresponding leaves.
3. Comparing across multiple plant–mycorrhizal fungus combinations, our data revealed metabolite alterations unique to mycorrhizal lifestyle as well as those common across plant–fungus combinations irrespective of lifestyles. Roots colonized by arbuscular mycorrhizal and ectomycorrhizal fungi accumulated different sets of carbohydrates, reflecting unique carbon allocation strategies for mycorrhizas. Arbuscular mycorrhizal roots accumulated cyclic polyols (e.g. inositol) inaccessible to their fungal partners, suggesting tight regulation of carbon partitioning. Such accumulation did not occur in ectomycorrhizal-colonized roots, which instead accrued acyclic polyols (e.g. mannitol and arabitol) that were undetected in non-mycorrhizal roots and likely of fungal origin. Mycorrhizas also altered specialized metabolism, featuring frequent increases in flavan-3-ols (e.g. catechins, gallicatechins, and their oligomers) but decreases in flavanols irrespective of mycorrhizal lifestyles, suggesting tactical reconfiguration of specialized metabolites

This is an open access article under the terms of the [Creative Commons Attribution](#) License, which permits use, distribution and reproduction in any medium, provided the original work is properly cited.

© 2022 The Authors. *Journal of Ecology* published by John Wiley & Sons Ltd on behalf of British Ecological Society.

to both facilitate and restrain the symbiont. These characteristic metabolite alterations were largely root specific and were not mirrored in leaves.

4. **Synthesis.** Using multiple plant–mycorrhizal systems and metabolomics approaches, our study demonstrates that part of the metabolite alterations occurring during root–mycorrhizal interactions were relatively common across plant–mycorrhizal systems, with implications for both carbon partitioning and tissue protection strategies important for successful symbiosis. These generalizable patterns appear robust to the phylogenetic history of host plants and thus may be widespread in land plants.

#### KEY WORDS

arbuscular mycorrhiza, carbohydrates, ectomycorrhiza, flavonoids, metabolomics, mycorrhizal roots, mycorrhizal symbiosis, plant–fungus interactions, polyols, primary metabolites

## 1 | INTRODUCTION

The vast majority of vascular plants in terrestrial ecosystems are involved in mycorrhizal symbioses (or mycorrhizas) with soil fungi, forming mycorrhizal roots, that is, hybrid below-ground organs containing both root and fungal tissues (Brundrett & Tedersoo, 2018). These widespread partnerships play a major role in shaping terrestrial ecosystems by mediating plant nutrition, plant responses to the environment and ecosystem biogeochemical cycles (Smith & Read, 2008). Thus, understanding the biological processes that underlie plant–mycorrhizal interactions is essential to the stewardship of the diverse array of ecosystem services provided by mycorrhizas, such as plant productivity, crop quality and ecosystem carbon (C) storage.

One common theme of plant–mycorrhizal interactions is convergent evolution (Genre et al., 2020; Miyauchi et al., 2020; Strullu-Derrien et al., 2018). About 50,000 soil fungal taxa with highly diverse evolutionary histories have converged into four main mycorrhizal lifestyles, among which arbuscular mycorrhizas (AMs) and ectomycorrhizas (EMs) dominate most terrestrial ecosystems (Brundrett & Tedersoo, 2018). The EM symbiosis has independently evolved ~80 times from multiple fungal lineages spanning an extended geological time period yet has converged to exhibit shared morphological root structures (e.g. external mantle) and intercellular Hartig net (Tedersoo & Smith, 2017). In contrast, the AM symbiosis does not exhibit a shared effect on root morphology but consistently results in the formation of intracellular arbuscules or hyphal coils in root cortical cells (Smith & Read, 2008). At the genome level, both AM and EM fungi share common traits such as lack/loss of lignin–cellulose degrading enzymes and expansion of functionally similar small-secreted protein families, some of which have been shown to counteract plant defence (Kloppholz et al., 2011; Plett et al., 2014). These convergent patterns within or across mycorrhizal lifestyles in morphological and genomic traits have been recently reviewed (Genre et al., 2020) and reflect common selection forces that define mycorrhizas.

Despite a growing understanding of trait convergence in mycorrhizas, the extent to which the mycorrhizal-associated metabolome

alterations may be shared within or across mycorrhizal lifestyles remains largely unexplored. Compared to genomic and transcriptomic traits, the metabolome represents the intermediates/end products of cellular regulation and thereby is closer to the phenotype produced by the gene–environmental interactions (Feussner & Polle, 2015; Fiehn, 2002). As such, the metabolome in plants and their symbiotic partners may also face direct selection pressures to sustain mycorrhizas and thus be subject to convergent alterations in response to shared challenges.

Plant–mycorrhizal interactions have been shown to reprogram the plant metabolome as a prerequisite for the establishment of functional mycorrhizas (e.g. Gaude et al., 2015, primary metabolites; Kaur et al., 2022, specialized metabolites), yet few studies have compared mycorrhizal-associated metabolite alterations across the plant and fungal species. A seminal study showed that multiple plant species colonized by the same AM fungus *Rhizophagus irregularis* exhibited little commonality but high plant species specificity in the leaf metabolome (Schweiger et al., 2014). However, leaf chemistry appears to be less affected by mycorrhizas than roots that directly accommodate mycorrhizal fungi (Xia et al., 2021). To our knowledge, comparisons of mycorrhizal-associated metabolite alterations in roots across multiple plant and fungal species or mycorrhizal lifestyles have yet to be attempted, partly because metabolites are highly diversified and metabolite studies often focused on different subsets of compounds. Such information will help uncover the potentially convergent biological processes that are important for functional mycorrhizas.

In this study, we sought to compare the metabolome of mycorrhizal and non-mycorrhizal roots across various combinations of plant hosts and mycorrhizal fungal species. We first asked if distinct metabolite alterations would align with different mycorrhizal lifestyles. AM and EM lifestyles are often linked with contrasting plant functions and ecosystem biogeochemical processes (e.g. Chen et al., 2016; Phillips et al., 2013). Prior studies suggest that AM and EM had different C partitioning patterns (Soudzilovskaia et al., 2015; van der Heijden et al., 2015). For example, estimates of photosynthate allocation suggest that <10% of photosynthetically fixed C is typically allocated to AM fungi

(Řezáčová et al., 2017, 2018), while EM fungi can receive up to 20–36% of fixed C (Bryla & Eissenstat, 2005; Hobbie, 2006; Řezáčová et al., 2017). AM and EM lifestyles were also shown to have differential reciprocal relationships, with greater C investment below-ground linked with higher nitrogen (N) uptake in AM-associated plants, whereas this positive relationship was not observed in EM plants, and high C investment often corresponded to low N return (Keller & Phillips, 2019). Collectively, these observations suggest that EM fungi possibly represent a stronger C sink, while C efflux from plant hosts to AM fungi may be more under plant control. This functional difference may be reflected in carbohydrate profiles, as fine-tuning of carbohydrates represents a means to mediate C partitioning between plants and fungi. For example, EM fungi in functional symbiosis quickly transformed hexoses to large amounts of fungal carbohydrates (Nehls et al., 2007; Plett et al., 2021), which may help maintain a sharp gradient at the exchange site and thus facilitate hexose efflux from plants to fungi (e.g. through a concentration-dependent transporter family, An et al., 2019). Accordingly, we hypothesized that (H1) AM and EM associations would differentially alter the carbohydrate profiles, reflecting their distinct C partitioning strategies. Particularly, we predicted that EM-colonized roots would maintain a greater proportional abundance of fungal-specific carbohydrates than AM roots, thereby maintaining a continuous, strong C sink.

We next asked if there are common metabolite alterations that frequently occur in mycorrhizas irrespective of mycorrhizal lifestyles, reflecting important shared selection forces shaping plant–mycorrhizal interactions. A common evolutionary trend of mycorrhizas is the expression of functionally similar genes in fungi, for example, small-secreted proteins that could dampen plant defence (Genre et al., 2020). Consistently, both AM and EM lifestyles have been shown to elicit only transient transcriptomic responses linked to plant defence/stress responses, which were later attenuated in established symbiosis (Giovannetti et al., 2015; Tarkka et al., 2013). If these genetic/transcriptional traits could be translated to chemistry/metabolite alterations, one would expect no or low level of defence/stress related specialized compounds in established mycorrhizal roots. This is supported by observations that the established mycorrhizal roots were associated with decreased or unaffected levels of protective compounds (e.g. cell-wall bound ferulic acids, tannins, Münzenberger et al., 1995; Solaiman & Senoo, 2018; Sebastian et al., 2021) and lack of additional lignin deposition (Chen et al., 2021). However, mycorrhizas were shown to accumulate defence compounds in the endodermis/exodermis of roots (e.g. Weiss et al., 1999), with these compartments proposed as being crucial in the evolution of mycorrhizas by forming barriers to detrimental fungal penetration (Brundrett, 2002; Strullu-Derrien et al., 2018). These seemingly contradictory patterns reflect a common requisite for mycorrhization: Roots must both facilitate and delimit the growth of symbiotic fungi. This general selection may result in convergent metabolite modulation. Accordingly, we hypothesized that (H2) the mycorrhizal-associated metabolite alterations would exhibit common patterns across

AM and EM lifestyles, reflecting chemical events critical for root–mycorrhizal fungal interactions. Specifically, the suppression of a subset of defence compounds to facilitate symbiosis would be accompanied by an upregulation of a different subset of specialized compounds which could be important for protecting root tissues in the presence of fungal colonization.

We tested these two primary hypotheses by characterizing the metabolome of mycorrhizal and non-mycorrhizal roots and their respective leaves in multiple plant–mycorrhizal fungus combinations across phylogenetically diverse temperate tree species forming either AM or EM associations. Using comprehensive metabolomics approaches, our data uncovered novel metabolome traits unique to a particular mycorrhizal lifestyle or common to both lifestyles, with implications for C partitioning and tissue protection strategies that could be critical for functional mycorrhizas.

## 2 | MATERIALS AND METHODS

### 2.1 | Greenhouse experiments

Two angiosperm and two gymnosperm species, with one species in each group forming AM and the other forming EM symbiosis were included in this study, to compare the potential role of phylogenetic relationship versus mycorrhizal lifestyle on shaping metabolite alterations (Table 1). We inoculated each of these host plant species with multiple fungal species to assess how responses may differ across plant–fungus combinations. All plants were grown in the Plant Growth Facilities greenhouse at the University of Minnesota (UMN), USA. The seeds of AM-associating *Juniperus virginiana* (JUVI) and *Liriodendron tulipifera* (LITU), and the EM-associating *Pinus taeda* (PITA) were purchased from Sheffield's Seed Company. The EM-associating *Quercus macrocarpa* (QUMA) was collected on the UMN campus grounds. The AM fungal inoculums *Gigaspora margarita* (Gm) and *Funneliformis mosseae* (Fm) were purchased from MycoBloom (MycoBloom LLC). The EM fungal inoculums included *Suillus brevipes* (Sb), *Suillus luteus* (Sl), *Thelephora terrestris* (Tt), *Laccaria* sp. (Ls) and *Tuber* sp. (Ts). Spores for the EM inoculums were prepared from field-collected sporocarps with spore slurries made following Mujic et al. (2016), with a small section of gleba being subjected to DNA extraction for species identification.

Seeds for all hosts but QUMA were placed on cloth beds, covered with cloth, dipped in 8% H<sub>2</sub>O<sub>2</sub> for 30 min, and soaked with H<sub>2</sub>O for 24 h. The bedded seeds were incubated at 4°C for stratification before sowing. For QUMA, germinated acorns with radicals not penetrating the soil were collected and rinsed with a 10% bleach solution before sowing. The soil (50:50 mix of quartz sand and natural soil from the Cedar Creek Ecosystem Science Reserve) was autoclaved and added to 70%-ethanol-sterilized trays, 2.5 L for each. We autoclaved the soil to limit the interference from preexisting organisms. However, this process may change soil chemistry and thus caution should be taken in generalizing the autoclaved soil to other soil systems. Inoculums were added at a

**TABLE 1** Mycorrhizal colonization rate, seedling height and the ratio of carbon and nitrogen (C/N) of roots and leaves from non-mycorrhizal and mycorrhizal seedlings

Host tree species	Tree abbr.	Fungal inoculum	Fungus abbr.	Biological replicates	Colonization (%)	Height (cm)	C/N (root)	C/N (leave)
AM								
<i>Juniperus virginiana</i> (gymnosperm)	JUVI	Non-mycorrhizal	NM	9	0 <sup>a</sup>	2.30 <sup>a</sup> ± 0.79	50.52 <sup>c</sup> ± 7.06	27.63 <sup>b</sup> ± 2.92
		<i>Funneliformis mosseae</i>	Fm	9	72.92 <sup>b</sup> ± 6.34	8.47 <sup>c</sup> ± 2.65	28.70 <sup>a</sup> ± 4.07	22.12 <sup>a</sup> ± 5.16
		<i>Gigaspora margarita</i>	Gm	9	67.59 <sup>b</sup> ± 10.14	6.64 <sup>b</sup> ± 2.22	33.96 <sup>b</sup> ± 3.80	29.65 <sup>b</sup> ± 4.67
<i>Liriodendron tulipifera</i> (angiosperm)	LITU	Non-mycorrhizal	NM	8	0 <sup>a</sup>	2.46 <sup>a</sup> ± 0.35	17.40 <sup>a</sup> ± 1.96	
		<i>Funneliformis mosseae</i>	Fm	9	75.37 <sup>b</sup> ± 10.13	5.83 <sup>b</sup> ± 3.48	24.81 <sup>b</sup> ± 3.93	
		<i>Gigaspora margarita</i>	Gm	5	72.67 <sup>b</sup> ± 9.40	4.49 <sup>b</sup> ± 1.63	29.45 <sup>c</sup> ± 5.28	
EM								
<i>Pinus taeda</i> (gymnosperm)	PITA	Non-mycorrhizal	NM	11	0 <sup>a</sup>	4.67 <sup>a</sup> ± 1.02	36.55 ± 5.29	38.59 <sup>b</sup> ± 8.91
		<i>Suillus brevipes</i>	Sb	10	44.76 <sup>c</sup> ± 14.82	6.42 <sup>bc</sup> ± 1.70	34.31 ± 2.55	31.47 <sup>ab</sup> ± 3.10
		<i>Suillus luteus</i>	Sl	3	5.96 <sup>b</sup> ± 2.84	5.55 <sup>b</sup> ± 0.88	33.81 ± 0.70	28.25 <sup>a</sup> ± 1.51
		<i>Sordariales</i> sp.	Ss	5	74.61 <sup>d</sup> ± 23.88	4.88 <sup>ab</sup> ± 1.01	37.52 ± 6.99	28.66 <sup>a</sup> ± 9.63
<i>Quercus macrocarpa</i> (angiosperm)	QUMA	Non-mycorrhizal	NM	8	0 <sup>a</sup>	7.98 ± 2.88	41.08 <sup>b</sup> ± 6.97	23.78 ± 5.20
		<i>Tuber</i> sp.	Ts	6	30.15 <sup>b</sup> ± 21.10	6.88 ± 2.25	31.98 <sup>a</sup> ± 4.73	25.75 ± 7.33

Note: The values are shown as mean ± SD. The effects of fungal inoculation were tested using one way ANOVA when the homogeneity of variance is met in all cases (Levene's test,  $p > 0.163$ ) except for the height of LITU (Levene's test,  $p = 0.001$ ), for which Kruskal-Wallis test was used. Different letters in the same column indicate significant differences within each plant species ( $p < 0.05$ ).

rate of 10% v/v. The two AM hosts were each inoculated with Gm and Fm; the two EM hosts were each inoculated with Ts and Ls, with PITA additionally inoculated with Tt, Sb and Sl. All mycorrhizal fungi were added as separate, single-species inoculums in separate trays. Each plant-fungus combination was represented in three trays along with three noninoculated trays for each host species. Turf Partners fertilizer was applied at the lowest recommended concentration monthly to each tray. Seedlings of JUVI and LITU were harvested after 7 months of growing, while PITA and QUMA were harvested at 9 and 11 months respectively.

During harvest, plant height (from the soil surface to apical meristem) for each seedling was recorded. Leaves and absorptive roots were collected from three to five individuals in each tray, and roots were separated into two subsamples for chemical and mycorrhizal analyses. The samples for chemical analysis were flash frozen in liquid N<sub>2</sub> and stored at -80°C until shipping to Clemson University with dry ice. The samples to be scored for colonization were stored in 60% ethanol. The remaining leaf and root material in each tray were oven-dried at 35°C. Root materials were collected for DNA analysis to confirm fungal identity.

## 2.2 | Mycorrhizal colonization and identity

Samples stored in 60% ethanol were washed in dH<sub>2</sub>O before scoring. AM-inoculated roots were cleared by 10% KOH and

autoclaved for a 60-min liquid cycle. After being rinsed with dH<sub>2</sub>O and acidified using 2.5% HCl, root samples were stained with Trypan Blue solution and set to autoclave for another 60-min cycle. Colonization of each seedling was quantified using gridline-intersect method (Giovannetti & Mosse, 1980). For EM colonization, all root tips in each seedling were scored under a dissecting microscope. In the Ls treatments for PITA and QUMA, and Ts for PITA, only a trace amount of colonization was present, so they were excluded from chemical analysis. The colonization of PITA roots by Sl was also low (~6%) but included for chemical analysis, as this low colonization resulted in an improved growth (Table 1). Low EM colonization (~2%) was also shown in a prior study to promote plant growth and modify plant metabolites (Szuba et al., 2020). We note that the chemical alterations observed in PITAxSl should be interpreted with caution due to the small sample size and low colonization.

Molecular identification of EM fungal identities was done by extracting DNA using the REDExtract-N-Amp protocol (Sigma-Aldrich). PCR using the fungal-specific primer pair ITS1F-ITS4 was conducted using the thermocycling conditions (Kennedy et al., 2020). PCR products were cleaned with Exo-SAP IT (USB Corp.) and sequenced in forward direction with the ITS1F primer at the UMN Genomics Center. Sequences were queried against the NCBI database to ascertain fungal identity. The Sb, Sl and Ts treatments matched closely (>99% similarity) to the inoculums, but the EM root tips in the Tt treatment matched closely to a *Sordarialean*

EM fungus previously encountered in arctic EM vegetation surveys (Brevik et al., 2010). Since colonization by this fungus was significant (~74.6% by average, Table 1), we included this treatment (coded as Ss) in chemical analysis.

## 2.3 | Chemical analysis

To correctly link chemical changes to colonization by each fungal inoculum, chemical analysis was performed on individual plants exhibiting significant colonization by identified fungal species. Accordingly, seedlings from the three trays for each of the JUVIxGm, JUVIxFm, LITUxFm, PITAxSb combinations were included in chemical analysis (biological replicates  $n = 9$ –10, Table 1). Colonization only occurred in two trays for the LITUxFm ( $n = 5$ ) and QUMAxTs pairs ( $n = 6$ ), and in one tray for the PITAxSs pair ( $n = 5$ ) and the PITAxSl pair ( $n = 3$ ). Colonization was not present in non-mycorrhizal controls ( $n = 8$ –11). Chemical analysis was performed for mycorrhizal, non-mycorrhizal roots and their corresponding leaves, except for LITU seedlings where only roots were analysed as we did not collect sufficient leaf material for chemical analysis. Because mycorrhizal roots contain both fungal and root tissues, we note that the metabolites detected in mycorrhizal roots cannot be unambiguously assigned to plants or fungi.

For metabolite profiling, 20 mg freeze-dried and cryohomogenized samples were extracted with 500  $\mu$ l methanol under sonication for 1 h in ice. The homogenate was centrifuged and 50  $\mu$ l methanol extracts were used for instrument analysis. The samples as well as method blanks (methanol) and quality control samples (QC, pooled extracts from all samples) were spiked with a 50- $\mu$ l internal standard (1  $\mu$ g ml<sup>−1</sup> resveratrol, 99 atom % <sup>13</sup>C<sub>6</sub>, Sigma-Aldrich), and analysed on an Ultimate 3000 HPLC (UHPLC, Thermo Scientific) with Acuity UPLC HSS T3 column (150  $\times$  2.1 mm, 1.8  $\mu$ m; Waters Corp.). The separated compounds were then analysed on a Orbitrap Fusion Tribrid Mass Spectrometer (UHPLC-Orbitrap-MS/MS, Thermo Scientific, Method S1). We processed the MS files with Compound Discoverer 3.2 (Thermo Scientific) for feature extraction, alignment and elemental composition prediction, with a mass tolerance of 5 ppm and S/N threshold at 5. The intensity of the extracted features in blanks were subtracted from those in samples. QC samples (injected at the interval of ~10 samples) are well aggregated in the PCoA of mass features (i.e. m/z signals detected as single peaks in the chromatogram, Figure S1), indicating consistency across UHPLC-Orbitrap-MS/MS analysis. After correcting for multiple adduct formation, the workflow extracted 7264 to 12,440 mass features across the four plant species. The elemental ratios were used to construct van Krevelen diagrams with expected biomolecular regions based on the constraints of O:C and H:C ratios (Kim et al., 2003; Rivas-Ubach et al., 2018). Putative compound-level annotations were based on matching the accurate mass (<5 ppm) of the precursor ions (MS1) and MS<sup>n</sup> fragmentation using the mzCloud database (match score > 80) and/or based on the accurate mass of the precursors and characteristic MS2 ions published in the literature (see annotations details for each compound in Table S1).

Because the number of compound-level annotations is limited compared to total mass features (<1%) and may bias towards a few well-characterized compounds documented in the published mass spectral libraries, we additionally assigned the mass features to multiple-level chemical taxonomy ClassyFire (Superclass, Class, Subclass, and Level 5, Djoumbou Feunang et al., 2016), using a computational tool CANOPUS (Dührkop et al., 2021). We first processed UHPLC-MS/MS files in MZmine 2.53, which, after peak picking, alignment and deisotoping, extracted features with MS2 scans (1118–2293 features across plant species). The extracted features were exported to SIRIUS (4.8.2) for the CANOPUS procedure that uses a deep neural network to predict compound classes from MS2 fragmentation. The ClassyFire classes determined by CANOPUS will be referred to as CANOPUS-assigned chemical classes in this study. We note that a small fraction (3%–6% across plant species) of the MZmine-extracted features can be annotated at the compound level using the mzCloud database/literature. Their ClassyFire classes were directly assigned based on their compound annotations and integrated to CANOPUS-assigned chemical classes. Overall, CANOPUS-assigned chemical classes cover a significant proportion of MZmine-extracted features at class level (e.g. phenol lipids, flavonoids, tannins): 71% to 88% (818 to 1402 features), across the four plant species. The robustness of data processing workflow and CANOPUS classification was verified by analysing and processing data from 242 authentic flavonoid standards.

We performed a separate metabolite profiling using a GC-QTOF system to better characterize polar metabolites that cover most of the primary metabolites (e.g. soluble carbohydrates, amino acids and organic acids). For the primary metabolite analysis, 200  $\mu$ l methanol extract was phase separated in a chloroform–water–methanol system (Lisec et al., 2006). Twenty microlitre water–methanol phase from each sample was spiked with a 10- $\mu$ l internal standard (50  $\mu$ g ml<sup>−1</sup> myristic acid +20  $\mu$ g ml<sup>−1</sup> ribitol) and dried under vacuum. The dried samples were methoximated with 20  $\mu$ l Methoxyamine-HCl (40 mg ml<sup>−1</sup> in pyridine) and derivatized by 80  $\mu$ l MSTFA +1% TMCS with 1  $\mu$ g mL<sup>−1</sup> alkanes (C10–C34) before being analysed on a gas chromatography-quadrupole time of flight mass spectrometer (GC-QTOF-MS, Agilent 7250, Agilent Technologies, Method S1). A standard of 38 authentic compounds were also analysed along with the samples. The GC-QTOF-MS files were processed with MS-DIAL 4.48 (Tsugawa et al., 2015) for peak detection, alignment and deconvolution. The annotations were based on matching the Kovats retention index (n-alkanes standards, C10–C34) and mass spectra to the MS-DIAL metabolomics database, with a part of these annotations further confirmed by authentic compounds or the literature (Table S1). Carbon and N concentrations were determined by a Carlo Erba Elemental Analyser at Duke University.

## 2.4 | Data analysis

Data analysis was performed with R software (version 4.0.3) unless otherwise stated. For the principal coordinates analysis (PCoA),

the dissimilarity index matrix (Euclidean) was constructed using the function `vegdist` from the `VEGAN` package after data standardization. Then, the function `pcoa` from the package `APE` was used to compute the principal coordinate decomposition of this distance matrix. We performed PERMANOVA to test the differences between treatments based on the Euclidean distances for the first three major PCoA axes using the function `adonis2` from the package `VEGAN`. PERMDISP was then performed on the same Euclidean distances to assess the homogeneity of dispersion using the function `betadisper`. The pairwise comparison (mycorrhizal vs. non-mycorrhizal) of chemical features was examined by a two-tailed Student's *t* test on the log-transformed peak intensities. The significance of differences in the log-transformed colonization rates, plant heights and N levels was tested with one-way ANOVA followed by post hoc comparisons. However, when the homogeneity of variance assumptions was not met, Kruskal–Wallis tests were performed to examine the main effect, followed by Mann–Whitney *U* tests for pairwise comparison. The variance partitioning that compared the potential drivers of the alterations in metabolites abundances followed the Legendre method (Legendre & Legendre, 2012) after data standardization, using the function `varpart` from package `VEGAN`. Data were log-transformed before statistical analysis. This procedure largely improved the homogeneity of variance for *t* tests (Table S2) and ANOVA (Table 1), which are robust to unequal sample sizes when the homogeneity of variance is met (De Winter, 2013; Harwell et al., 1992). We used Levene's tests corrected for structural zeros that are robust to variable sample sizes to test homogeneity of variance (Noguchi & Gel, 2010; Parra-Frutos, 2013). The pathway (KEGG) analysis was performed with PaintOomics 3 (v0.4.5, based on *Arabidopsis thaliana*, García-Alcalde et al., 2011) using Fisher exact tests to test the significant changes on pathways.

### 3 | RESULTS

#### 3.1 | Mycorrhizal colonization, plant growth and nutrient status

AM fungi Gm and Fm colonized JUVI and LITU roots at high and consistent levels (67.6%–75.4%, Table 1). Colonization by EM was variable, typically ranging from 30% to 75%. Mycorrhizal colonization improved plant growth and/or the levels of N (gauged by the ratio of C and N, C/N) across all plant–fungus combinations, indicating functional symbiosis. Specifically, the seedlings of JUVI, LITU and PITA exhibited improved growth by two mycorrhizal fungal species (Table 1). Although colonization by Ss and Ts did not result in a better growth for PITA and QUMA, respectively, it led to a lower C/N (thus higher N levels) in either their leaves or roots (Table 1). Because metabolites may also depend on plant growth and nutrient utilization, we performed variance partitioning analysis to compare the potential drivers (mycorrhizal colonization, plant growth and/or N) of metabolite alterations in the following analysis.

#### 3.2 | Global changes of the metabolome

Mycorrhizal roots had a different metabolome than their non-mycorrhizal counterparts in all plant–fungus combinations (Figure 1). A large number of mass features in roots were detected by UHPLC–Orbitrap-MS/MS followed by Compound Discoverer, ranging from 7264 to 12,440 features across plant species (Table S2), albeit 120,000 resolution (at *m/z* 200), of which 87% to 93% were assigned with molecular formulas at <5 ppm mass tolerance. Among the features assigned with formulas, AM differentially regulated 4494 to 7231 features (i.e. features that differentiate between mycorrhizal vs. non-mycorrhizal roots), while EM changed 1288 to 3439 features (*p* < 0.05, Figure 1a). These altered features are distributed across a broad range of chemical space defined by O:C and H:C ratios and span all predicted compounds categories. The difference in the number of altered features between AM and EM were not likely due to the difference in colonization rate. For example, AM fungus Fm and EM fungus Ss exhibited similar colonization rates (~70%) in LITU and PITA, respectively (Table 1), but Fm altered twofold more features in LITU than Ss in PT (Figure 1a). However, the colonization rates of AM and EM may not be comparable due to their different counting methods (i.e. length based vs. root tip based respectively).

Considering the overall chemical landscape, PCoA showed that the four plant species separated into distinct chemical phenotypes, with two gymnosperms closer to each other and further away from the two angiosperms (Figure S2), mirroring their phylogenetic relationships more than mycorrhizal similarities. Within each plant species, colonized roots exhibited a different chemistry from those uncolonized (PERMANOVA *p* < 0.028, PERMANOVA *r*<sup>2</sup> ranges from 0.18 to 0.88, Figure 1b), and their differences were more driven by the shift in chemical phenotype than the dissimilarity of within-group variations as the dispersion was relatively homogeneous across different mycorrhizal inoculums and their non-mycorrhizal controls (PERMDISP *p* > 0.126, Figure 1b). Not only did the chemical phenotypes differ between colonized versus uncolonized roots, roots from the same plant species that were colonized by different fungal species also separated into distinct clusters (Figure 1b), indicating that the mycorrhizal-associated metabolite alterations were significant and specific to fungal species. Together, these observations demonstrated significant global metabolic alterations by mycorrhizas in all plant–fungus combinations in this study and set the stage for understanding common versus unique metabolome traits across plant–mycorrhizal systems.

#### 3.3 | Alterations of primary metabolism

The GC-QTOF-MS revealed that mycorrhizas altered major groups of primary metabolites such as amino acids, organic acids and carbohydrates (further grouped as disaccharides, pentoses, hexoses and polyols, a carbohydrate derivative, Figure 2a, Figure S3). AM associations and the PITAxSb combination exhibited notable changes in

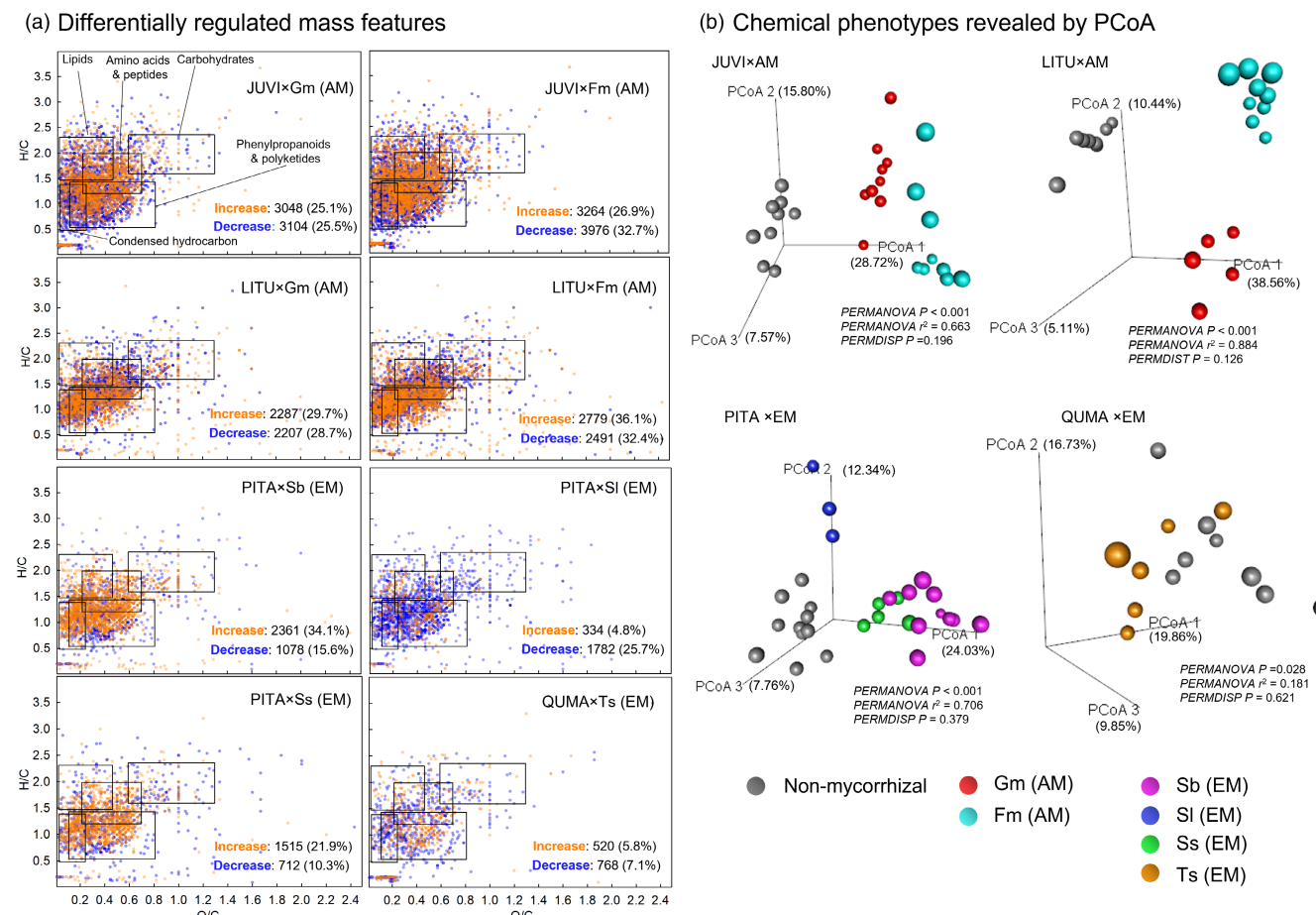


**FIGURE 1** Mycorrhizal-associated changes in the chemical landscapes of roots across eight plant–mycorrhizal fungus combinations. (a) Van Krevelen diagrams show the distribution of differentially regulated metabolites (mycorrhizal vs. non-mycorrhizal, Student's  $t$  test,  $p < 0.05$ ) in expected biomolecular regions. (b) Principal coordinates analysis (PCoA) shows the separation of chemical phenotypes between non-mycorrhizal and mycorrhizal roots colonized by different fungal species based on the first three major PCoA components. The significance of separation is indicated by PERMANOVA  $p$  values, with the effect size indicated by PERMANOVA  $r^2$  values. PERMDISP  $p > 0.050$  indicates homogeneity of dispersion. See Table 1 for abbreviations.

most primary metabolite groups, whereas other EM pairings showed more scattered responses (Figure 2a).

Mycorrhizas frequently affected carbohydrate profiles (Figure 2a–c, Figure S3). The pathway analysis detected significant alterations in several sugar metabolism pathways, with galactose metabolism exhibiting modification in six of eight plant–fungus combinations (Table S3). Particularly, the abundance of sugars such as sucrose, glucose, fructose and mannose was frequently affected by symbiosis, but their responses were variable across plant–fungus combination (Figure 2b, Figure S3). For example, the responses of glucose and fructose, the two hexoses readily transportable from roots to mycorrhizal fungi, differed among plant species: AM decreased glucose and fructose in JUVI roots but increased these compounds in LITU; EM increased glucose and fructose in PITA roots but they were unaffected in QUMA (Figure 2b, Figure S3).

In contrast to the variable changes of sugars, we observed a similar trend in another major C pool, that is, polyols and their derivatives, within one mycorrhizal lifestyle (Figure 2b,c, Figure S3). In line with H1, AM and EM tended to affect polyols in different manners.

Arbuscular mycorrhizal-colonized roots accumulated cyclic polyols, that is, inositol and their methoxy derivatives such as ononitol and pinitol. This accumulation occurred in JUVI and LITU with AM lifestyles irrespective of the phylogenetic history of hosts (gymnosperm vs. angiosperm) or fungal identities (Gm vs. Fm). By contrast, EM-colonized roots did not exhibit similar increases in cyclic polyols but substantially accumulated a set of new compounds that were undetected or at trace levels in non-mycorrhizal roots, including acyclic polyols and trehalose (Figure 2b,c, Figure S3). The large increase in acyclic polyols in EM roots was driven by the accumulation of mannitol and arabitol in PITA and mannitol in QUMA (Figure S3), with these compounds contributing >90% of the increase. The PITA x Ss combination is the only pairing of EM association that did not accumulate acyclic polyols but instead exhibited a large increase in trehalose (Figure 2c).

Variance partitioning showed that the changes in carbohydrates were more related to colonization by mycorrhizal fungi than plant growth and tissue N (Figure S4). Overall, colonization explained 22%–64% of the variation in polyol profiles, with

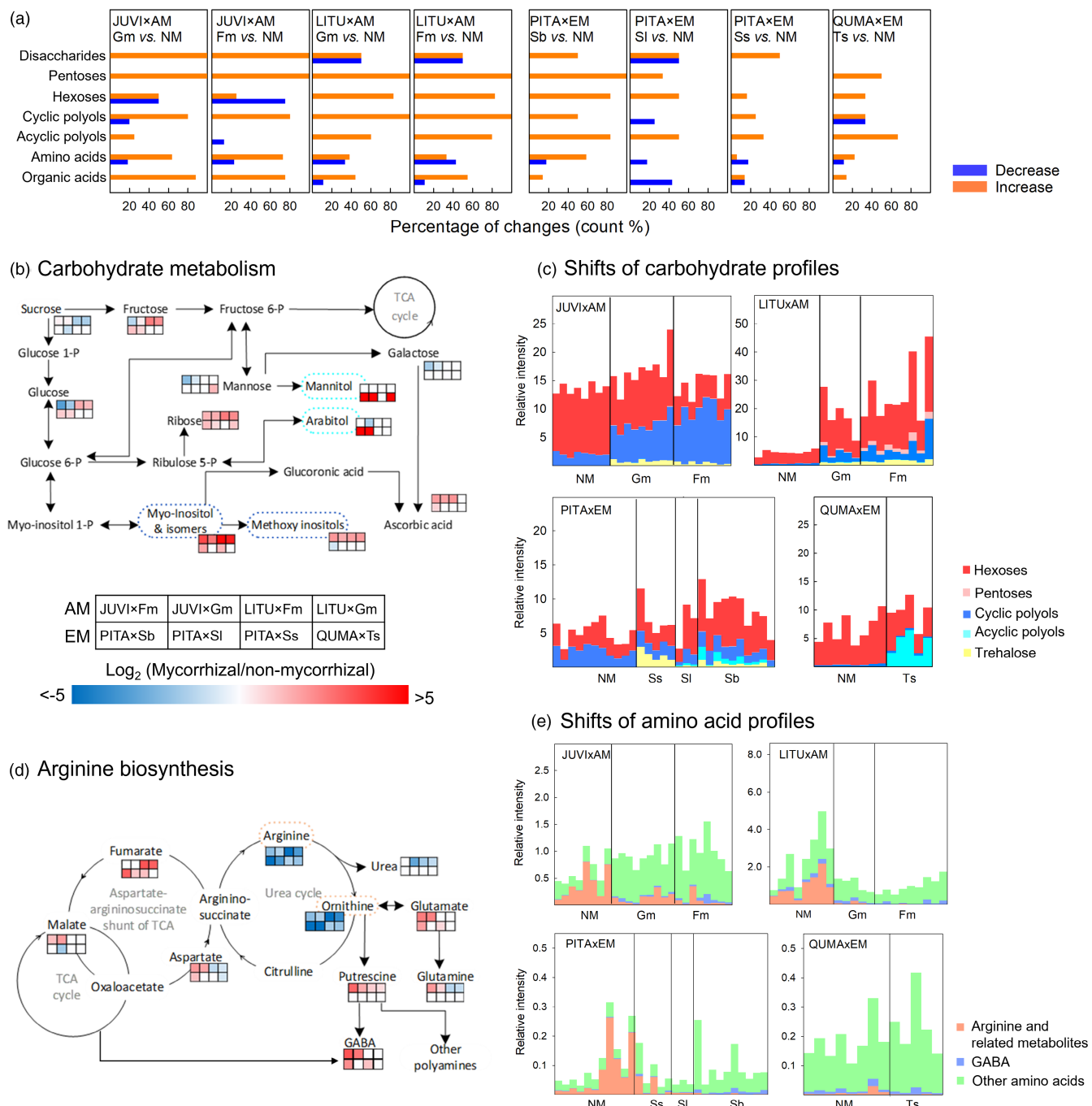


**FIGURE 2** Mycorrhizal-associated alterations in the primary metabolites of roots across eight plant-mycorrhizal fungus combinations. (a) Percentage of changes (mycorrhizal vs. non-mycorrhizal or NM, Student's *t* test,  $p < 0.05$ ) in primary metabolites. (b) Sugar metabolism simplified from KEGG primary pathways. (c) Shifts of carbohydrate profiles were shown by the summed relative intensity (normalized to the internal standard) of carbohydrates and polyols for individual seedlings. (d) Arginine biosynthesis pathway simplified from KEGG amino acid pathways. (e) Changes of amino acid profiles were shown by the summed relative intensity for individual seedlings. In (b) and (d), the compounds with significant differences ( $p < 0.05$ ) between mycorrhizal and NM roots in each of the eight plant-fungus combinations are shown in a gradient from red to blue based on the  $\log_2$  fold changes, with blank indicating nonsignificant effects or undetected compounds. See Table 1 for abbreviations.

9%–21% of the variation explained by mycorrhizas independently ( $p \leq 0.063$ ), whereas growth and N did not show significant net effects ( $p \geq 0.308$ ). To understand if the metabolic changes occurred in a systemic manner, we also investigated the abundance of polyols in the leaves for each plant-fungus combination. We observed

increases in cyclic polyols in leaves of AM-inoculated JUVI seedlings, although to a considerably lesser degree when compared to their below-ground counterparts (Figure 2c, Figure S5a). Acyclic polyols such as mannitol and arabitol were undetected or at trace levels in the leaves of EM-inoculated seedlings.

Mycorrhizas also altered amino acids and organic acids (Figure 2d,e, Figure S3). Although their changes were largely mixed, we observed a common trend where the abundance of arginine and its catabolism products was consistently decreased by mycorrhizas across most plant–fungus combinations irrespective of mycorrhizal lifestyles, leading to a characteristic shift of amino acid profiles. Pathway analysis also showed that arginine biosynthesis was sensitive to mycorrhizas and was altered by symbiosis in seven of eight plant–fungus combinations (Table S3). Particularly, metabolites involved in the urea cycle (arginine, ornithine and urea) were decreased in most plant–fungus combinations (Figure 2d,e), whereas the metabolites from their neighbouring pathways, for example, the biosynthesis of polyamines and  $\gamma$ -aminobutyric acid (GABA, a stress-related nonprotein amino acid), tended to increase, indicating C flow away from the urea cycle (Figure 2d,e). Tissue N and mycorrhizal colonization are important factors explaining the changes in arginine and related metabolites, with tissue N independently explained 18%–31% of the variation across the four plant species (Figure S4). The decrease in arginine and related metabolites also occurred in the leaves of mycorrhizal-associated seedlings (Figure S5b).

### 3.4 | Alterations of specialized metabolism

The CANOPUS-assigned chemical classes were used to characterize the broad responses of the specialized metabolism in roots. This procedure revealed a similar distribution of the metabolome at high levels of chemical classes across plant species (Figure 3a). At the superclass level, the metabolome from all plant species was dominated by organic acids and derivatives, organic oxygen compounds, lipids and like, and phenylpropanoids and polyketides. Flavonoids were consistently a major group of phenylpropanoids and polyketides, whereas prenol lipids and fatty acyls comprised the majority of lipids and like. This broad similarity provides opportunities for understanding potential commonality versus specificity of metabolite alterations. The metabolome in roots also exhibited plant species-specific traits, especially at finer levels. For example, The CANOPUS-assigned phenylpropanoids were dominated by flavonoids in PITA roots, LITU roots produced similar numbers of flavonoids and hydroxycinnamic acids and derivatives, while QUMA roots were abundant in hydrolysable tannins (Figure 3).

Most of the CANOPUS-assigned specialized metabolite groups exhibited changes due to mycorrhizas (Figure 3b). In general, AM tended to elicit higher numbers and greater proportions of changes than EM. Among the specialized metabolite groups, the CANOPUS-assigned phenylpropanoids exhibited the highest numbers of changes (Figure 3b). The responsiveness of phenylpropanoids was relatively consistent across plant–fungus combinations: although EM roots were in general less responsive than AM roots, the EM fungi Sb and SI still elicited a high number (169 to 189) and large proportion (50.0% to 55.9%) of responses in the CANOPUS-assigned phenylpropanoids of PITA roots. By contrast, while the prenol lipids showed a high response to AM (particularly, diterpenoids in JUVI

and terpene glycosides in LITU), EM elicited considerably lower proportions of responses in this chemical group (Figure 3b).

The high response of the CANOPUS-assigned phenylpropanoids to mycorrhizas was predominantly driven by the changes in the CANOPUS-assigned flavonoids, which accounted for 86.4%, 42.5%, 90.8% and 70.1% of the observed responses of phenylpropanoids in JUVI, LITU, PITA and QUMA respectively (Figure 3b). Accordingly, we focused on flavonoids and related metabolites because: (1) this chemical family was highly responsive to mycorrhizas; (2) flavonoids are almost exclusively synthesized by plants. Our survey across the genome sequences of the studied fungal species/genus (i.e. Gm, Sb, SI and Ts) suggests that none of these fungi possesses the essential enzyme kit (ammonia-lyase, chalcone synthase and chalcone isomerase, Winkel, 2006) required in the flavonoid biosynthesis (database: MycoCosm, Grigoriev et al., 2014). Although we did not separate plant from fungal metabolites, the relative exclusiveness of flavonoids allows for elucidating modulation of plant metabolites without confounding changes by fungal metabolism. In addition, (3) the core pathway of flavonoid metabolism is largely shared across the plant kingdom (Wen et al., 2020), allowing for comparing its response across plant–fungus systems.

Next, we assessed the mycorrhiza-associated changes in the specialized metabolites that were annotated at the compound level based on the mzCloud database/literature, which broadly cover the phenylpropanoid, flavonoid and the adjacent metabolism pathways (Figure 4a, see annotation details in Table S1 and the respective response of each compound in Table S4). Pathway analysis showed that flavonoid biosynthesis was frequently affected by mycorrhizas across plant–fungus combinations (Table S3). Comparing specialized metabolite alterations across plant–fungus combinations revealed concerted, yet differential responses between two major flavonoid subgroups. The members of a flavonoid subgroup, flavonols (quercetins, kaempferols, myricetins and their derivatives), exhibited mixed, largely decreasing responses to mycorrhizas (Figure 4, Table S4). By contrast, we observed a consistent increase in the members of another flavonoid subgroup, that is, flavan-3-ols (e.g. catechins, gallicatechins and their oligomers such as procyanidins and prodelphinidins, Figure 4, Table S4), leading to a pronounced increase in the summed peak intensities of this group in seven of eight plant–fungus combinations ( $p < 0.001$ , Figure 4b). The frequent accumulation of flavan-3-ols along with the general decrease in other flavonoids resulted in a characteristic shift of flavonoid profiles by mycorrhizas in most plant–fungus combinations irrespective of mycorrhizal lifestyles (Figure 4b). The only exception is the PITAxSI pairing, where the colonization rate was the lowest among plant–fungus combinations (~6%, Table 1). Mapping annotated compounds to the flavonoid biosynthesis pathway showed that mycorrhizas tended to drive C flow towards later steps of the flavonoid biosynthesis pathway, as flavan-3-ols are synthesized further downstream than flavonols (Figure 4b). Mycorrhizal colonization was the most important predictor for the changes in flavan-3-ols, explaining 56%–85% of the variation, with 9%–81% of the variation explained independently (Figure S4). A similar accumulation of flavan-3-ols did not occur in

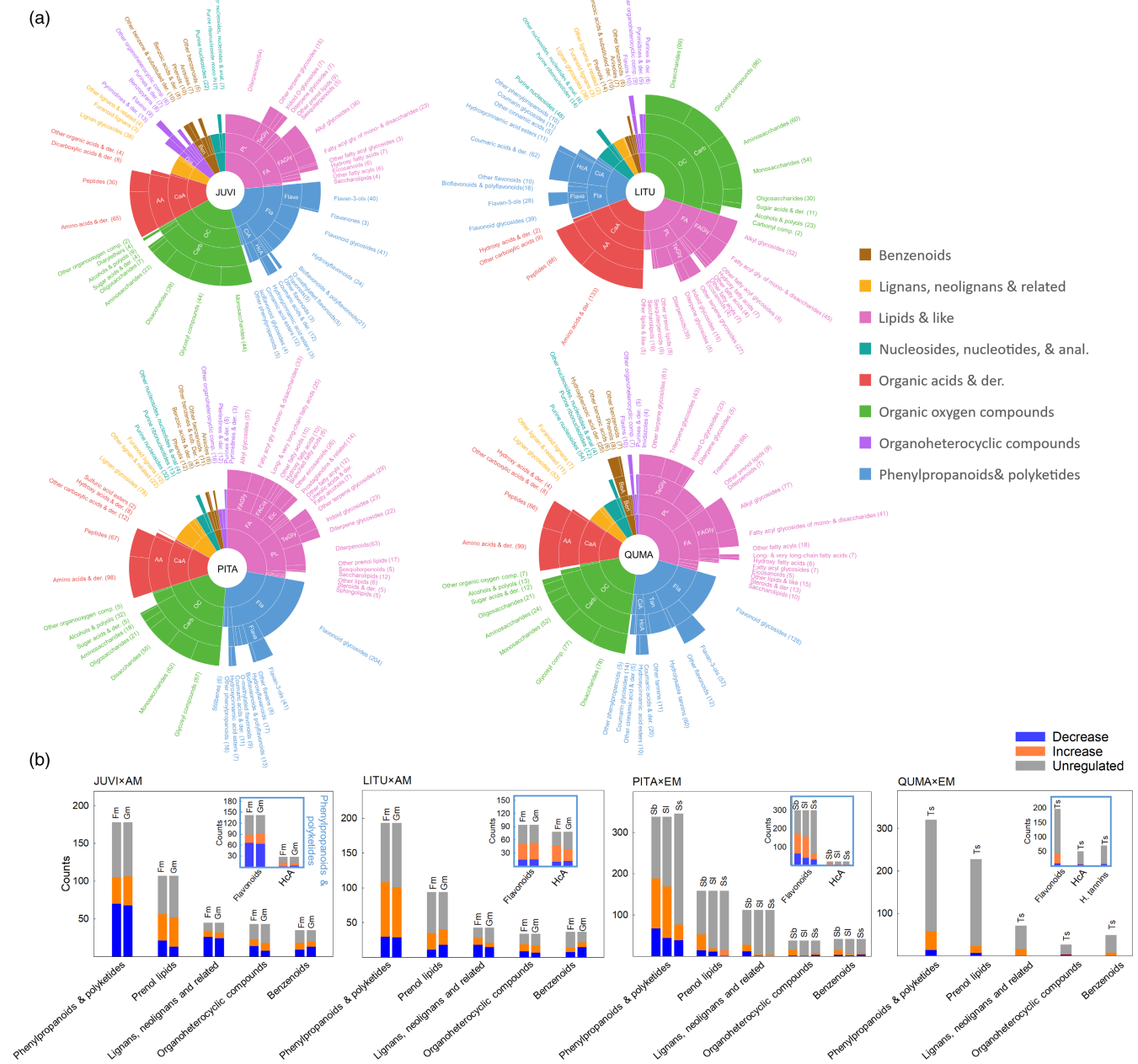


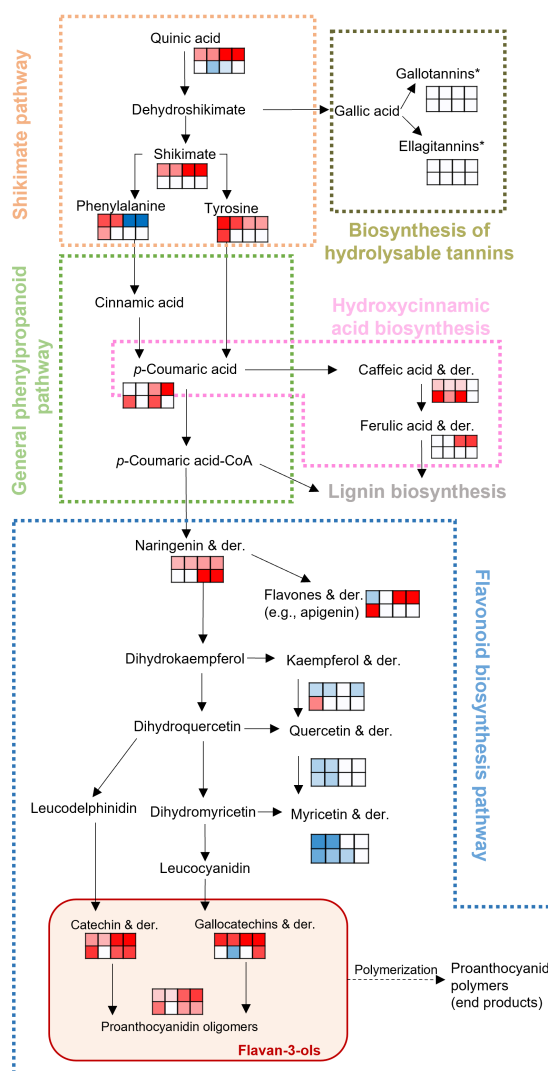
**FIGURE 3** Variation in the specialized metabolites of roots across eight plant–mycorrhizal fungus combinations. (a) The proportions of the CANOPUS-assigned chemical classes at four taxonomy levels (from superclass, class, subclass, to level 5 outward) across four plant species. AA: Amino acids, peptides and analogues; BeA: Benzenoid acids and derivatives (der.); ben: Benzene and substituted der.; CaA: Carboxylic acids and der.; carb: Carbohydrates and conjugates; CiA: Cinnamic acids and der.; Dia: Diazines; Eic: Eicosanoids; FA: Fatty acyls; FAGly: Fatty acyl glycosides (gly.); Fla: Flavonoids; flava: Flavans; HcA: Hydroxycinnamic acids and der.; OC: Organoxygen compounds (comp.); PL: Prenol lipids; tan: Tannins; TeGly: Terpene gly. Groups with features  $<2$  were combined for better comprehensibility. (b) The counts of altered (mycorrhizal vs. non-mycorrhizal, Student's *t* test,  $p < 0.05$ ) and unregulated features that are assigned by CANOPUS to specialized metabolite groups. The insets show the changes ( $p < 0.05$ ) of the subgroups in phenylpropanoids and polyketides. H. Tannins: Hydrolysable tannins. See Table 1 for abbreviations of plant and fungal species.

leaves: The presence of below-ground mycorrhizas decreased or did not affect the summed peak intensities of flavan-3-ols in leaves (Figure S5).

Because the number of annotations is limited compared to that of unannotated mass features, we further tested if this characteristic shift of flavonoid profiles is robust to a broader range of the

CANOPUS-assigned flavonoids. Similarly, the CANOPUS-assigned flavonols exhibited mixed and largely decreasing responses to mycorrhizas; by contrast, we observed frequent increases in the CANOPUS-assigned flavan-3-ols (Figure S6a,b). The summed peak intensities of the assigned flavan-3-ols increased by mycorrhizas in seven of eight plant–fungus combinations, whereas that

(a) Phenylpropanoid, flavonoid &amp; related pathways



(b) Characteristic shift of flavonoid profiles by mycorrhizas

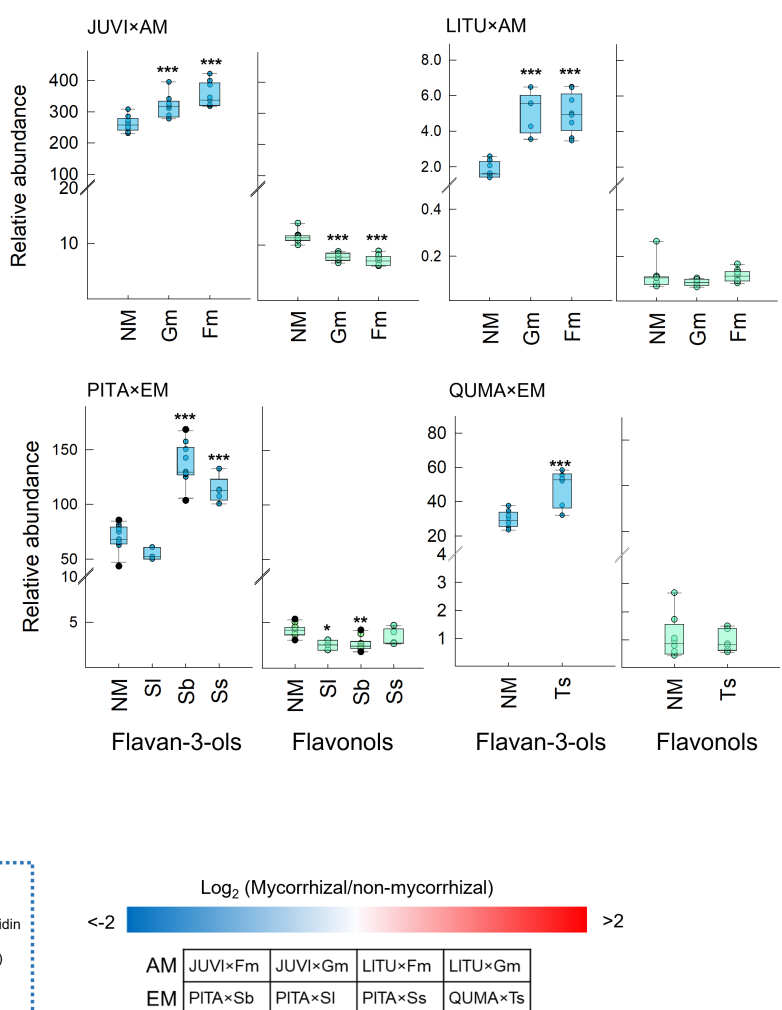


**FIGURE 4** Mycorrhizal-associated shifts in the flavonoid profiles of roots across eight plant–mycorrhizal fungus combinations. (a) Flavonoid biosynthesis simplified from KEGG pathways. Compounds with significant differences (Student's *t* test,  $p < 0.05$ ) between mycorrhizal and non-mycorrhizal (NM) roots are shown in a gradient from red to blue based on the  $\log_2$  fold changes, with blank indicating nonsignificant effects or undetected compounds. \*Gallotannins and ellagitannins were only detected in QUMA roots and were unaffected by mycorrhizas. (b) Characteristic shifts of flavonoid profiles by mycorrhizas featured by the differential changes in the summed intensity (normalized to internal standards) between flavan-3-ols and flavonols. \*:  $p < 0.05$ ; \*\*:  $p < 0.01$ ; \*\*\*:  $p < 0.001$ . See Table 1 for abbreviations.

of the features assigned as other flavonoids generally decreased (Figure S6c). These patterns of the CANUPUS-assigned classes further support the shift of flavonoid profiles (i.e. accumulation of flavan-3-ols) as a characteristic alteration of specialized metabolites associated with mycorrhizas irrespective of mycorrhizal lifestyles.

## 4 | DISCUSSION

Characterizing chemical landscapes associated with diverse root–mycorrhizal interactions, our data showed that the mycorrhizal-associated metabolite alterations were complex, involving decreases

and increases in a large number of metabolites spanning major chemical classes. However, using a multi-species approach, common versus lifestyle-specific metabolite alterations across plant–mycorrhizal fungus combinations emerged. Although metabolite responses are often considered specific to plant/fungal species (Schweiger et al., 2014), our data demonstrated that part of the mycorrhizal-associated metabolite alterations were relatively common across plant–mycorrhizal systems. This commonality is particularly striking as it persisted irrespective of the phylogenetic relationships among host plants and appeared robust to the variable mycorrhizal-mediated changes on plant growth and N status.

The common metabolite alterations by mycorrhizas may reflect selection pressures and biological processes critical for successful

mycorrhizas. For example, carbohydrate partitioning between plant hosts and fungal partners is fundamental for successful symbiosis, as carbohydrates (hexoses in particular), along with lipids, are the currencies that plants use for exchange with fungi (Keymer et al., 2017; Shachar-Hill et al., 1995). Mutualistic mycorrhizal associations would require well-regulated C partitioning between plants and fungi (Brundrett, 2002). Such a general requirement may result in convergent alterations in carbohydrate profiles. However, the responses of the immediately exchangeable hexoses (e.g. glucose, fructose) were highly variable across plant–fungus combinations, reflecting dynamic nature of these readily transportable carbohydrates. On the other hand, our data revealed that polyols, a major C pool in root tissues, frequently accumulated in mycorrhizal roots. The two AM hosts, although phylogenetically and chemically distinct from each other, both accumulated cyclic polyols (i.e. inositol and derivatives). Inositol typically have a plant origin (the BioBase database, Lai et al., 2018) and significant amounts of inositol were also detected in uninoculated roots and leaves. Accumulating large amounts of cyclic polyols that are less available for symbionts may help plants to mitigate the hexose gradient at the root–fungus interface and thus regulate carbohydrate efflux to AM fungi (Nehls et al., 2007; Nehls & Bodendiek, 2012). In line with our observation, at the cellular level, inositol are among the most responsive carbohydrates to AM: arbuscule-containing cells accumulated inositol while hexoses were generally unaffected (Gaude et al., 2015). A recent study also showed that accumulation of inositol was pronounced in mutualistic AM associations but was lacking when AM fungi exhibited a parasitic phenotype (Kaur et al., 2022). These and our observations collectively suggest that accumulation of inositol may be a common C partitioning strategy in AM-associated roots and open intriguing questions on the potential regulatory role of this frequent accumulation, for example, a possible avenue for plants to regulate C exchange to AM symbionts.

In contrast to AM roots, and consistent with H1, EM-associated roots accumulated a different set of polyols (i.e. acyclic polyols such as mannitol and arabitol) that often have a fungal origin and may have different biological consequences. Our findings are consistent with prior observations that EM fungi can produce large amounts of mannitol and/or arabitol (Nehls & Bodendiek, 2012) and that EM fungi quickly transformed hexoses to large quantities of mannitol, accounting for up to >60% of total fungal carbohydrates (Lewis & Harley, 1965; Nehls et al., 2007; Nehls & Bodendiek, 2012). The EM plant host PITA does not naturally produce mannitol, which have motivated prior studies to genetically modify this species to enable mannitol synthesis for stress tolerance (e.g. Tang et al., 2005). In addition, mannitol and arabitol were undetected in uninoculated roots. Therefore, their frequent accumulation in EM roots was more likely driven by fungal metabolism. In contrast to the accumulation of inositol that may help plant roots regulate C efflux, quickly converting hexoses to acyclic polyols may instead help EM fungi maintain a strong sink for carbohydrates at the exchange site and facilitate hexose efflux from plants to symbionts. Interestingly, accumulation of mannitol/arabitol has also been observed in fungal pathogens

as important for pathogenicity, with proposed functions such as carbohydrate reserves and quenchers for plant ROS responses (Hooshmand et al., 2020; Patel & Williamson, 2016). This similarity between EM and pathogens implicates an evolutionary scenario where the accumulation of these acyclic polyols is crucial for the establishment of fungal colonization in host tissues. Taken together, the contrasting alterations in carbohydrate profiles between AM and EM lifestyles reflect their unique C partitioning strategies for sustaining symbiosis and provide potential mechanisms driving the divergent C utilization between different lifestyles.

Alterations of specialized metabolites that regulate plant defence to biotic/abiotic stresses also represent an essential step for mycorrhization (Kaur & Suseela, 2020). To facilitate symbiosis, plant defence responses were often suppressed as a result of decreased expression of defence-related genes (Zamioudis & Pieterse, 2012). On the other hand, plants need to limit the undesirable spread of fungi. This modulation is likely through altering nonstructural specialized metabolites, as symbiosis may precede significant lignin/suberin deposition in root endodermis that form physical barriers (Brundrett, 2002). Therefore, the general challenges of mycorrhization (facilitation vs. delimitation) could be translated into complex alterations in specialized metabolites.

Our data showed that a large specialized metabolite group, flavonoids, are highly responsive to mycorrhizas. The core steps of flavonoid biosynthesis pathway are largely conserved (Wen et al., 2020), which may allow for convergent responses to mycorrhizas across plant species. Indeed, comparing across plant–fungus combinations revealed a characteristic shift in flavonoid profiles that occurred frequently in mycorrhizal-colonized roots irrespective of lifestyles. In line with H2, this shift featured general decreases in flavonols but increases in flavan-3-ols, which may be interpreted in the context that plants facilitate and delimitate mycorrhizal fungal growth. Flavonols and derivatives exhibited a variable, generally decreasing trend in colonized roots. Such mixed responses suggest that they may have versatile functions. Indeed, while flavonols are thought to have antifungal activity (Sudheeran et al., 2020) and thus at odds with mycorrhizas, certain flavonols can instead stimulate mycorrhizas and positively relate to colonization (Lagrange et al., 2001). In contrast, the family of flavan-3-ols showed a consistent accumulation across plant–fungus combinations irrespective of mycorrhizal lifestyles. These increases were unique to roots and did not occur in leaves, indicating a potential regulatory role of this flavonoid subgroup in root–fungus interactions. Flavan-3-ols are among the most potent flavonoids to defend against fungal penetration (Friedman, 2007; Ullah et al., 2019). Flavan-3-ols such as catechins were observed to accumulate in large quantities in the inner part of root endodermis in *Larix decidua* Mill. (Weiss et al., 1999) and cotton seedlings (Mace & Howell, 1974), forming critical barriers against fungal inward growth to vascular tissues. Interestingly, a similar strategy was observed in Plant-*Frankia* symbiosis as *Frankia*-infected cells were delimited by cell layers with elevated levels of flavan-3-ols (Laplace et al., 1999). Hence, the general accumulation of flavan-3-ols in mycorrhizal roots may represent a common defence investment of plant hosts

to prevent undesirable fungal penetration. Moreover, the protective role of flavan-3-ols may be multi-level. Many members of this group are efficient ROS scavengers that trap an additional peroxy radical compared to other flavonoids (Kondo et al., 2000). Their antioxidant properties may further protect plant tissues from fungal-induced ROS responses. Imaging analyses that examine the localization of flavan-3-ols in mycorrhizal roots could further elucidate their protective roles for mycorrhizal-associated plants. The accumulation of flavan-3-ols in mycorrhizal roots may also have ecological consequences as specialized metabolites can influence litter decomposition (Chomel et al., 2016; Cornelissen et al., 2022).

The common metabolite responses observed in roots were largely localized and were not mirrored in leaves. This may explain the lack of commonality across plant species in leaf metabolic responses to *Rhizophagus irregularis* (Schweiger et al., 2014). Leaves are not the immediate site of mycorrhization, nor do they directly face the challenges that could shape root chemistry in similar ways and lead to convergent alterations (e.g. delimiting undesirable fungal spread). However, symbiosis could induce systemic changes that indirectly affect leaf chemistry. For example, the decrease in arginine and related metabolites occurred in both roots and leaves. Because the variations of these compounds were related to tissue N, their changes in leaves may be driven by mycorrhizal-associated systemic changes in plant N utilization. Our data demonstrated that mycorrhizas tend to have different relationships to root and leaf chemistry and thus the transferability of the findings in the metabolic alterations by mycorrhizas from roots to leaves (and vice versa) is limited.

In conclusion, we have demonstrated common and mycorrhizal lifestyle-specific traits of metabolite alterations across various plant–mycorrhizal fungus combinations. Although many metabolites (e.g. hexoses, flavonols) showed mixed alterations that were specific to plant species and/or fungal identities, a subset of highly responsive compounds (e.g. polyols and flavan-3-ols) exhibited responses to mycorrhizas that were, in some cases, shared across both mycorrhizal lifestyles, and were in other cases unique to a given lifestyle. These observations open intriguing questions on their potentially important regulatory and evolutionary role for successful symbiosis.

## AUTHOR CONTRIBUTIONS

All authors contributed to conceptualizing the research idea and study design. M. Luke McCormack and Peter G. Kennedy performed the greenhouse experiment, collected the samples and performed analysis for mycorrhizal identification and colonization. Mengxue Xia and Nishanth Tharayil performed chemical analysis. Mengxue Xia performed data analysis and wrote the draft of the manuscript with critical feedbacks from M. Luke McCormack, Peter G. Kennedy, Vidya Suseela and Nishanth Tharayil.

## ACKNOWLEDGEMENTS

This research is supported by funding from the grants (DEB 1754679 and 1753621) from the U.S. National Science Foundation. Part of the analysis was supported by The National Institute of Food and

Agriculture award 2021-70410-35296 to the Multi-User Analytical Laboratory at Clemson University. This is technical contribution No. 7109 of the Clemson University Experiment Station.

## CONFLICT OF INTEREST

The authors have no conflict of interest to declare.

## PEER REVIEW

The peer review history for this article is available at <https://publon.com/publon/10.1111/1365-2745.14049>.

## DATA AVAILABILITY STATEMENT

The metabolomics dataset obtained from UHPLC-Orbitrap-MS/MS has been deposited to MassIVE Repository (MSV000090615, <https://doi.org/10.25345/C5JH3D69S>). The MS dataset obtained from QTOF-GC-MS (primarily for primary metabolites) has been deposited to MassIVE Repository (MSV000090616, <https://doi.org/10.25345/C5DR2PD64>).

## ORCID

Mengxue Xia  <https://orcid.org/0000-0003-4366-3253>

Vidya Suseela  <https://orcid.org/0000-0002-2934-4849>

M. Luke McCormack  <https://orcid.org/0000-0002-8300-5215>

Peter G. Kennedy  <https://orcid.org/0000-0003-2615-3892>

Nishanth Tharayil  <https://orcid.org/0000-0001-6866-0804>

## REFERENCES

An, J., Zeng, T., Ji, C., de Graaf, S., Zheng, Z., Xiao, T. T., Deng, X., Xiao, S., Bisseling, T., Limpens, E., & Pan, Z. (2019). A *Medicago truncatula* SWEET transporter implicated in arbuscule maintenance during arbuscular mycorrhizal symbiosis. *New Phytologist*, 224, 396–408. <https://doi.org/10.1111/nph.15975>

Brevik, A., Moreno-Garcia, J., Wenefczyk, J., Blaalid, R., Eidesen, P. B., & Carlsen, T. (2010). Diversity of fungi associated with *Bistorta vivipara* (L.) Delarbre root systems along a local chronosequence on Svalbard. *Agarica*, 29, 15–26.

Brundrett, M. C. (2002). Coevolution of roots and mycorrhizas of land plants. *New Phytologist*, 154, 275–304. <https://doi.org/10.1046/j.1469-8137.2002.00397.x>

Brundrett, M. C., & Tedersoo, L. (2018). Evolutionary history of mycorrhizal symbioses and global host plant diversity. *New Phytologist*, 220, 1108–1115. <https://doi.org/10.1111/nph.14976>

Bryla, D. R., & Eissenstat, D. M. (2005). Respiratory costs of mycorrhiza associations. In H. Lambers & M. Ribas-Carbo (Eds.), *Plant respiration* (pp. 207–224). Springer.

Chen, M., Bruisson, S., Bapaume, L., Darbon, G., Glauser, G., Schorderet, M., & Reinhardt, D. (2021). VAPYRIN attenuates defence by repressing PR gene induction and localized lignin accumulation during arbuscular mycorrhizal symbiosis of *Petunia hybrida*. *New Phytologist*, 229, 3481–3496. <https://doi.org/10.1111/nph.17109>

Chen, W., Koide, R. T., Adams, T. S., DeForest, J. L., Cheng, L., & Eissenstat, D. M. (2016). Root morphology and mycorrhizal symbioses together shape nutrient foraging strategies of temperate trees. *Proceedings of the National Academy of Sciences of the United States of America*, 113, 8741–8746. <https://doi.org/10.1073/pnas.16010061>

Chomel, M., Guittonny-Larchevêque, M., Fernandez, C., Gallet, C., DesRochers, A., Paré, D., Jackson, B. G., & Baldy, V. (2016). Plant

secondary metabolites: A key driver of litter decomposition and soil nutrient cycling. *Journal of Ecology*, 104, 1527–1541. <https://doi.org/10.1111/1365-2745.12644>

Cornelissen, J. H. C., Cornwell, W. K., Freschet, G. T., Weedon, J. T., Berg, M. P., & Zanne, A. E. (2022). Coevolutionary legacies for plant decomposition. *Trends in Ecology & Evolution*. In press. <https://doi.org/10.1016/j.tree.2022.07.008>

De Winter, J. C. (2013). Using the Student's t-test with extremely small sample sizes. *Practical Assessment, Research, and Evaluation*, 18, 10. <https://doi.org/10.7275/e4r6-dj05>

Djoumbou Feunang, Y., Eisner, R., Knox, C., Chepelev, L., Hastings, J., Owen, G., Fahy, E., Steinbeck, C., Subramanian, S., Bolton, E., & Greiner, R. (2016). ClassyFire: Automated chemical classification with a comprehensive, computable taxonomy. *Journal of Cheminformatics*, 8, 1–20. <https://doi.org/10.1186/s1332-1-016-0174-y>

Dührkop, K., Nothias, L. F., Fleischauer, M., Reher, R., Ludwig, M., Hoffmann, M. A., Petras, D., Gerwick, W. H., Rousu, J., Dorrestein, P. C., & Böcker, S. (2021). Systematic classification of unknown metabolites using high-resolution fragmentation mass spectra. *Nature Biotechnology*, 39, 462–471. <https://doi.org/10.1038/s41587-020-0740-8>

Feussner, I., & Polle, A. (2015). What the transcriptome does not tell—Proteomics and metabolomics are closer to the plants' patho-phenotype. *Current Opinion in Plant Biology*, 26, 26–31. <https://doi.org/10.1016/j.pbi.2015.05.023>

Fiehn, O. (2002). Metabolomics—The link between genotypes and phenotypes. *Functional Genomics*, 48, 155–171. [https://doi.org/10.1007/978-94-010-0448-0\\_11](https://doi.org/10.1007/978-94-010-0448-0_11)

Friedman, M. (2007). Overview of antibacterial, antitoxin, antiviral, and antifungal activities of tea flavonoids and teas. *Molecular Nutrition & Food Research*, 51, 116–134. <https://doi.org/10.1002/mnfr.200600173>

García-Alcalde, F., García-López, F., Dopazo, J., & Conesa, A. (2011). Paintomics: A web based tool for the joint visualization of transcriptomics and metabolomics data. *Bioinformatics*, 27, 137–139. <https://doi.org/10.1093/bioinformatics/btq594>

Gaude, N., Bortfeld, S., Erban, A., Kopka, J., & Krajinski, F. (2015). Symbiosis dependent accumulation of primary metabolites in arbuscule-containing cells. *BMC Plant Biology*, 15, 1–9. <https://doi.org/10.1186/s12870-015-0601-7>

Genre, A., Lanfranco, L., Perotto, S., & Bonfante, P. (2020). Unique and common traits in mycorrhizal symbioses. *Nature Reviews Microbiology*, 18, 649–660. <https://doi.org/10.1038/s4159-020-0402-3>

Giovannetti, M., Mari, A., Novero, M., & Bonfante, P. (2015). Early *Lotus japonicus* root transcriptomic responses to symbiotic and pathogenic fungal exudates. *Frontiers in Plant Science*, 6, 480. <https://doi.org/10.3389/fpls.2015.00480>

Giovannetti, M., & Mosse, B. (1980). An evaluation of techniques for measuring vesicular arbuscular mycorrhizal infection in roots. *New Phytologist*, 84, 489–500.

Grigoriev, I. V., Nikitin, R., Haridas, S., Kuo, A., Ohm, R., Otiillar, R., Riley, R., Salamov, A., Zhao, X., Korzeniewski, F., & Smirnova, T. (2014). MycoCosm portal: Gearing up for 1000 fungal genomes. *Nucleic Acids Research*, 42, 699–704. <https://doi.org/10.1093/nar/gkt1183>

Harwell, M. R., Rubinstein, E. N., Hayes, W. S., & Olds, C. C. (1992). Summarizing Monte Carlo results in methodological research: The one-and two-factor fixed effects ANOVA cases. *Journal of Educational Statistics*, 17, 315–339. <https://doi.org/10.3102/10769986017004315>

Hobbie, E. A. (2006). Carbon allocation to ectomycorrhizal fungi correlates with belowground allocation in culture studies. *Ecology*, 87, 563–569. <https://doi.org/10.1890/05-0755>

Hooshmand, K., Kudjordjie, E. N., Nicolaisen, M., Fiehn, O., & Fomsgaard, I. S. (2020). Mass spectrometry-based metabolomics reveals a concurrent action of several chemical mechanisms in *arabidopsis-fusarium oxysporum* compatible and incompatible interactions. *Journal of Agricultural and Food Chemistry*, 68, 15335–15344. <https://doi.org/10.1021/acs.jafc.0c05144>

Kaur, S., Campbell, B. J., & Suseela, V. (2022). Root metabolome of plant–arbuscular mycorrhizal symbiosis mirrors the mutualistic or parasitic mycorrhizal phenotype. *New Phytologist*, 234, 672–687. <https://doi.org/10.1111/nph.17994>

Kaur, S., & Suseela, V. (2020). Unraveling arbuscular mycorrhiza-induced changes in plant primary and secondary metabolome. *Metabolites*, 10, 335. <https://doi.org/10.3390/metabo10080335>

Keller, A. B., & Phillips, R. P. (2019). Relationship between belowground carbon allocation and nitrogen uptake in saplings varies by plant mycorrhizal type. *Frontiers in Forests and Global Change*, 2, 81. <https://doi.org/10.3389/ffgc.2019.00081>

Kennedy, P. G., Gagne, J., Perez-Pazos, E., Lofgren, L. A., & Nguyen, N. H. (2020). Does fungal competitive ability explain host specificity or rarity in ectomycorrhizal symbioses? *PLoS One*, 15, e0234099. <https://doi.org/10.1371/journal.pone.0234099>

Keymer, A., Pimprikar, P., Wewer, V., Huber, C., Brands, M., Bucerius, S. L., Delaux, P. M., Klingl, V., von Roepenack-Lahaye, E., Wang, T. L., & Eisenreich, W. (2017). Lipid transfer from plants to arbuscular mycorrhiza fungi. *eLife*, 6, e29107. <https://doi.org/10.7554/eLife.29107>

Kim, S., Kramer, R. W., & Hatcher, P. G. (2003). Graphical method for analysis of ultrahigh-resolution broadband mass spectra of natural organic matter, the van Krevelen diagram. *Analytical Chemistry*, 75, 5336–5344. <https://doi.org/10.1021/ac034415p>

Kloppholz, S., Kuhn, H., & Requena, N. (2011). A secreted fungal effector of *Glomus intraradices* promotes symbiotic biotrophy. *Current Biology*, 21, 1204–1209. <https://doi.org/10.1016/j.cub.2011.06.044>

Kondo, K., Kurihara, M., Fukuhara, K., Tanaka, T., Suzuki, T., Miyata, N., & Toyoda, M. (2000). Conversion of procyanidin B-type (catechin dimer) to A-type: Evidence for abstraction of C-2 hydrogen in catechin during radical oxidation. *Tetrahedron Letters*, 41, 485–488. [https://doi.org/10.1016/S0040-4039\(99\)02097-3](https://doi.org/10.1016/S0040-4039(99)02097-3)

Lagrange, H., Jay-Allmand, C., & Lapeyrie, F. (2001). Rutin, the phenolglycoside from eucalyptus root exudates, stimulates *Pisolithus* hyphal growth at picomolar concentrations. *New Phytologist*, 149, 349–355. <https://doi.org/10.1046/j.1469-8137.2001.00027.x>

Lai, Z., Tsugawa, H., Wohlgemuth, G., Mehta, S., Mueller, M., Zheng, Y., Ogiwara, A., Meissen, J., Showalter, M., Takeuchi, K., & Kind, T. (2018). Identifying metabolites by integrating metabolome databases with mass spectrometry cheminformatics. *Nature Methods*, 15, 53–56. <https://doi.org/10.1038/nmeth.4512>

Laplaze, L., Gherbi, H., Frutz, T., Pawlowski, K., Franche, C., Macheix, J. J., Auguy, F., Bogusz, D., & Duhoux, E. (1999). Flavan-containing cells delimit *Frankia*-infected compartments in *Casuarina glauca* nodules. *Plant Physiology*, 121, 113–122. <https://doi.org/10.1104/pp.121.1.113>

Legendre, P., & Legendre, L. F. (2012). *Numerical ecology*. Elsevier.

Lewis, D., & Harley, J. (1965). Carbohydrate physiology of mycorrhizal roots of beech: I. identity of endogenous sugars and utilization of exogenous sugars. *New Phytologist*, 64, 224–237. <https://doi.org/10.1111/j.1469-8137.1965.tb05393.x>

Lisec, J., Schauer, N., Kopka, J., Willmitzer, L., & Fernie, A. R. (2006). Gas chromatography mass spectrometry-based metabolite profiling in plants. *Nature Protocols*, 1, 387–396. <https://doi.org/10.1038/nprot.2006.59>

Mace, M., & Howell, C. (1974). Histochemistry and identification of condensed tannin precursors in roots of cotton seedlings. *Canadian Journal of Botany*, 52, 2423–2426.

Miyauchi, S., Kiss, E., Kuo, A., Drula, E., Kohler, A., Sánchez-García, M., Morin, E., Andreopoulos, B., Barry, K. W., Bonito, G., & Buée, M. (2020). Large-scale genome sequencing of mycorrhizal fungi provides insights into the early evolution of symbiotic traits. *Nature Communications*, 11, 1–17. <https://doi.org/10.1038/s41467-020-18795-w>

Mujic, A. B., Durall, D. M., Spatafora, J. W., & Kennedy, P. G. (2016). Competitive avoidance not edaphic specialization drives vertical niche partitioning among sister species of ectomycorrhizal fungi. *New Phytologist*, 209, 1174–1183. <https://doi.org/10.1111/nph.13677>

Münzenberger, B., Kottke, I., & Oberwinkler, F. (1995). Reduction of phenolics in mycorrhizas of *Larix decidua* mill. *Tree Physiology*, 15, 191–196. <https://doi.org/10.1093/treephys/15.3.191>

Nehls, U., & Bodendiek, I. (2012). 7 carbohydrates exchange between symbionts in ectomycorrhizas. In K. Esser (Ed.), *Fungal associations* (pp. 119–136). Springer.

Nehls, U., Grunze, N., Willmann, M., Reich, M., & Küster, H. (2007). Sugar for my honey: Carbohydrate partitioning in ectomycorrhizal symbiosis. *Phytochemistry*, 68, 82–91. <https://doi.org/10.1016/j.phytochem.2006.09.024>

Noguchi, K., & Gel, Y. R. (2010). Combination of Levene-type tests and a finite-intersection method for testing equality of variances against ordered alternatives. *Journal of Nonparametric Statistics*, 22, 897–913. <https://doi.org/10.1080/10485251003698505>

Parra-Frutos, I. (2013). Testing homogeneity of variances with unequal sample sizes. *Computational Statistics*, 28, 1269–1297. <https://doi.org/10.1007/s00180-012-0353-x>

Patel, T. K., & Williamson, J. D. (2016). Mannitol in plants, fungi, and plant-fungal interactions. *Trends in Plant Science*, 21, 486–497. <https://doi.org/10.1016/j.tplants.2016.01.006>

Phillips, R. P., Brzostek, E., & Midgley, M. G. (2013). The mycorrhizal-associated nutrient economy: A new framework for predicting carbon-nutrient couplings in temperate forests. *New Phytologist*, 199, 41–51. <https://doi.org/10.1111/nph.12221>

Plett, J. M., Daguerre, Y., Wittulsky, S., Vayssières, A., Deveau, A., Melton, S. J., Kohler, A., Morrell-Falvey, J. L., Brun, A., Veneault-Fourrey, C., & Martin, F. (2014). Effector MiSSP7 of the mutualistic fungus *Laccaria bicolor* stabilizes the *Populus JAZ6* protein and represses jasmonic acid (JA) responsive genes. *Proceedings of the National Academy of Sciences of the United States of America*, 111, 8299–8304. <https://doi.org/10.1073/pnas.1322671111>

Plett, K. L., Kohler, A., Lebel, T., Singan, V. R., Bauer, D., He, G., Ng, V., Grigoriev, I. V., Martin, F., Plett, J. M., & Anderson, I. C. (2021). Intra-species genetic variability drives carbon metabolism and symbiotic host interactions in the ectomycorrhizal fungus *Pisolithus microcarpus*. *Environmental Microbiology*, 23, 2004–2020. <https://doi.org/10.1111/1462-2920.15320>

Řezáčová, V., Konvalinková, T., & Jansa, J. (2017). Carbon fluxes in mycorrhizal plants. In A. Varma, R. Prasad, & N. Tuteja (Eds.), *Mycorrhiza - ecology, secondary metabolites, nanomaterials* (pp. 1–21). Springer.

Řezáčová, V., Slavíková, R., Zemková, L., Konvalinková, T., Procházková, V., Štovíček, V., Hršelová, H., Beskid, O., Hujšlová, M., Gryndlerová, H., Gryndler, M., Püschel, D., & Jansa, J. (2018). Mycorrhizal symbiosis induces plant carbon reallocation differently in C3 and C4 *Panicum* grasses. *Plant and Soil*, 425, 441–456. <https://doi.org/10.1007/s11104-018-3606-9>

Rivas-Ubach, A., Liu, Y., Bianchi, T. S., Tolic, N., Jansson, C., & Pasa-Tolic, L. (2018). Moving beyond the van Krevelen diagram: A new stoichiometric approach for compound classification in organisms. *Analytical Chemistry*, 90, 6152–6160. <https://doi.org/10.1021/acs.analchem.8b00529>

Schweiger, R., Baier, M. C., Persicke, M., & Müller, C. (2014). High specificity in plant leaf metabolic responses to arbuscular mycorrhiza. *Nature Communications*, 5, 1–11. <https://doi.org/10.1038/ncomm5486>

Sebastiana, M., Gargallo-Garriga, A., Sardans, J., Pérez-Trujillo, M., Monteiro, F., Figueiredo, A., Maia, M., Nascimento, R., Silva, M. S., Ferreira, A. N., & Cordeiro, C. (2021). Metabolomics and transcriptomics to decipher molecular mechanisms underlying ectomycorrhizal root colonization of an oak tree. *Scientific Reports*, 11, 1–16. <https://doi.org/10.1038/s41598-021-87886-5>

Shachar-Hill, Y., Pfeffer, P. E., Douds, D., Osman, S. F., Doner, L. W., & Ratcliffe, R. G. (1995). Partitioning of intermediary carbon metabolism in vesicular-arbuscular mycorrhizal leek. *Plant Physiology*, 108, 7–15. <https://doi.org/10.1104/pp.108.1.7>

Smith, S. E., & Read, D. J. (2008). *Mycorrhizal symbiosis*. Academic Press.

Solaiman, Z. M., & Senoo, K. (2018). Arbuscular mycorrhizal fungus causes increased condensed tannins concentrations in shoots but decreased in roots of *Lotus japonicus* L. *Rhizosphere*, 5, 32–37. <https://doi.org/10.1016/j.rhisph.2017.11.006>

Soudzilovskaia, N. A., van der Heijden, M. G., Cornelissen, J. H., Makarov, M. I., Onipchenko, V. G., Maslov, M. N., Akhmetzhanova, A. A., & van Bodegom, P. M. (2015). Quantitative assessment of the differential impacts of arbuscular and ectomycorrhiza on soil carbon cycling. *New Phytologist*, 208, 280–293. <https://doi.org/10.1111/nph.13447>

Strullu-Derrien, C., Selosse, M. A., Kenrick, P., & Martin, F. M. (2018). The origin and evolution of mycorrhizal symbioses: From palaeomycology to phylogenomics. *New Phytologist*, 220, 1012–1030. <https://doi.org/10.1111/nph.15076>

Sudheeran, P. K., Ovadia, R., Galsarker, O., Maoz, I., Sela, N., Maurer, D., Feygenberg, O., Oren Shamir, M., & Alkan, N. (2020). Glycosylated flavonoids: fruit's concealed antifungal arsenal. *New Phytologist*, 225, 1788–1798. <https://doi.org/10.1111/nph.16251>

Szuba, A., Marczak, Ł., & Ratajczak, I. (2020). Metabolome adjustments in ectomycorrhizal *Populus × canescens* associated with strong promotion of plant growth by *Paxillus involutus* despite a very low root colonization rate. *Tree Physiology*, 40, 1726–1743. <https://doi.org/10.1093/treephys/tpaa100>

Tang, W., Peng, X., & Newton, R. J. (2005). Enhanced tolerance to salt stress in transgenic loblolly pine simultaneously expressing two genes encoding mannitol-1-phosphate dehydrogenase and glucitol-6-phosphate dehydrogenase. *Plant Physiology and Biochemistry*, 43, 139–146. <https://doi.org/10.1016/j.plaphy.2005.01.009>

Tarkka, M. T., Herrmann, S., Wubet, T., Feldhahn, L., Recht, S., Kurth, F., Mailaender, S., Boenn, M., Neef, M., Angay, O., & Bacht, M. (2013). OakContig DF 159.1, a reference library for studying differential gene expression in *Quercus robur* during controlled biotic interactions: Use for quantitative transcriptomic profiling of oak roots in ectomycorrhizal symbiosis. *New Phytologist*, 199, 529–540. <https://doi.org/10.1111/nph.12317>

Tedersoo, L., & Smith, M. E. (2017). Ectomycorrhizal fungal lineages: Detection of four new groups and notes on consistent recognition of ectomycorrhizal taxa in high-throughput sequencing studies. In L. Tedersoo (Ed.), *Biogeography of mycorrhizal symbiosis* (pp. 125–142). Springer.

Tsugawa, H., Cajka, T., Kind, T., Ma, Y., Higgins, B., Ikeda, K., Kanazawa, M., VanderGheynst, J., Fiehn, O., & Arita, M. (2015). MS-DIAL: Data-independent MS/MS deconvolution for comprehensive metabolome analysis. *Nature Methods*, 12, 523–526. <https://doi.org/10.1038/nmeth.3393>

Ullah, C., Unsicker, S. B., Reichelt, M., Gershenzon, J., & Hammerbacher, A. (2019). Accumulation of catechin and proanthocyanidins in black poplar stems after infection by *Plectosphaerella populi*: Hormonal regulation, biosynthesis and antifungal activity. *Frontiers in Plant Science*, 10, 1441. <https://doi.org/10.3389/fpls.2019.01441>

van der Heijden, M. G., Martin, F. M., Selosse, M. A., & Sanders, I. R. (2015). Mycorrhizal ecology and evolution: The past, the present, and the future. *New Phytologist*, 205, 1406–1423. <https://doi.org/10.1111/nph.13288>

Weiss, M., Schmidt, J., Neumann, D., Wray, V., Christ, R., & Strack, D. (1999). Phenylpropanoids in mycorrhizas of the Pinaceae. *Planta*, 208, 491–502. <https://doi.org/10.1007/s004250050586>

Wen, W., Alseckh, S., & Fernie, A. R. (2020). Conservation and diversification of flavonoid metabolism in the plant kingdom. *Current Opinion in Plant Biology*, 55, 100–108. <https://doi.org/10.1016/j.pbi.2020.04.004>

Winkel, B. S. (2006). The biosynthesis of flavonoids. In E. Grotewold (Ed.), *The science of flavonoids* (pp. 71–95). Springer.

Xia, M., Valverde-Barrantes, O. J., Suseela, V., Blackwood, C. B., & Tharayil, N. (2021). Coordination between compound-specific chemistry and morphology in plant roots aligns with ancestral mycorrhizal association in woody angiosperms. *New Phytologist*, 232, 1259–1271. <https://doi.org/10.1111/nph.17561>

Zamioudis, C., & Pieterse, C. M. (2012). Modulation of host immunity by beneficial microbes. *Molecular Plant-Microbe Interactions*, 25, 139–150. <https://doi.org/10.1094/MPMI-06-11-0179>

**How to cite this article:** Xia, M., Suseela, V., McCormack, M. L., Kennedy, P. G., & Tharayil, N. (2023). Common and lifestyle-specific traits of mycorrhizal root metabolome reflect ecological strategies of plant–mycorrhizal interactions. *Journal of Ecology*, 111, 601–616. <https://doi.org/10.1111/1365-2745.14049>

## SUPPORTING INFORMATION

Additional supporting information can be found online in the Supporting Information section at the end of this article.

### Supplementary Materials

Table S1, S4